

# Lawrence Berkeley National Laboratory

## Recent Work

### Title

K+n CHARGE EXCHANGE HEAR 1 GeV/c

### Permalink

<https://escholarship.org/uc/item/1kt753wj>

### Authors

Hirata, A.A.  
Goldhaber, G.  
Hall, B.H.  
et al.

### Publication Date

1971

0.2

$K^+$  n CHARGE EXCHANGE NEAR 1 GeV/c

A. A. Hirata, G. Goldhaber, B. H. Hall, V. H. Seeger,  
G. H. Trilling, and C. G. Wohl

January 12, 1971

AEC Contract No. W-7405-eng-48

**TWO-WEEK LOAN COPY**

*This is a Library Circulating Copy  
which may be borrowed for two weeks.  
For a personal retention copy, call  
Tech. Info. Division, Ext. 5545*

LAWRENCE RADIATION LABORATORY  
UNIVERSITY of CALIFORNIA BERKELEY

0.2

## **DISCLAIMER**

This document was prepared as an account of work sponsored by the United States Government. While this document is believed to contain correct information, neither the United States Government nor any agency thereof, nor the Regents of the University of California, nor any of their employees, makes any warranty, express or implied, or assumes any legal responsibility for the accuracy, completeness, or usefulness of any information, apparatus, product, or process disclosed, or represents that its use would not infringe privately owned rights. Reference herein to any specific commercial product, process, or service by its trade name, trademark, manufacturer, or otherwise, does not necessarily constitute or imply its endorsement, recommendation, or favoring by the United States Government or any agency thereof, or the Regents of the University of California. The views and opinions of authors expressed herein do not necessarily state or reflect those of the United States Government or any agency thereof or the Regents of the University of California.

$K^+n$  CHARGE EXCHANGE NEAR 1 GeV/c\*

A. A. Hirata,<sup>†</sup> G. Goldhaber, B. H. Hall,  
V. H. Seeger,<sup>‡</sup> G. H. Trilling, and C. G. Wohl<sup>#</sup>

Department of Physics and Lawrence Radiation Laboratory  
University of California, Berkeley, California 94720

January 12, 1971

Abstract: We present cross sections and angular distributions for the reaction  $K^+d \rightarrow K^0pp$  at 865, 970, 1210, 1365, and 1585 MeV/c.

Making corrections for deuterium effects, we observe the following features of the elastic charge exchange process  $K^+n \rightarrow K^0p$ : (a) the center-of-mass angular distribution becomes increasingly peripheral as the momentum increases from 800 to 1600 MeV/c; (b) the forward amplitude is largely real. Attempts to describe the data either in terms of a Regge model or in terms of dominance by an elastic  $P_{1/2}$  isoscalar KN resonance are discussed.

## 1. INTRODUCTION

High-precision measurements of  $K^+d$  and  $K^+p$  total cross sections in the momentum region around 500 to 1500 MeV/c have suggested the existence of rather interesting structure. Although disagreements between the results of various groups coupled with the uncertainties generated in the unfolding of deuterium effects preclude precise knowledge of the shape of the  $I = 0$  total cross section there is suggestive evidence for a very broad ( $\Gamma = 560$  MeV) nearly elastic resonance at a mass of 1780 MeV plus an additional peak, perhaps also interpretable as a resonance at about 1850 MeV, just above  $K^*$  threshold [1].

---

\*Work supported by the U. S. Atomic Energy Commission.

<sup>†</sup>Present address: Department of Natural Philosophy, University of Glasgow, Glasgow, Scotland.

<sup>‡</sup>Present address: Physics Department, San Francisco State College, San Francisco, California.

<sup>#</sup>Present address: Nuclear Physics Laboratory, Oxford University, Oxford, England.

The magnitude of the total cross section effectively limits the elastic resonance (if this interpretation is correct) to a  $J = 1/2$  state. Phase shift analyses already published indicate that the dominant  $I = 0$  wave is  $P_{1/2}$  [2]; this result is in agreement with measurements of the total cross section at very low energy [3]. Thus the natural resonance interpretation of the total cross-section structure in the 500-1000 MeV/c momentum region is in terms of a  $P_{1/2}$  state.

The next step in attempting to confirm or disprove this interpretation is to study elastic  $I = 0$  KN scattering. The analysis of elastic  $K^+n$  charge exchange is a particularly simple way of getting at some information on the isoscalar KN elastic processes.

As part of a program to study the  $K^+N$  interaction around 1 GeV/c, we have analyzed  $K^+d$  interactions at momenta of 865, 970, 1210, 1365, and 1585 MeV/c. In this paper we present the results of an analysis of the reaction



from which we deduce the principal features of the related  $K^+n$  charge exchange reaction



including cross sections and angular distributions. We have attempted to see if our results are compatible with a nearly elastic  $P_{1/2}$  wave resonating at a mass of about 1780 MeV, and have also made comparisons with the low energy extrapolation of a Regge model developed for higher energy interactions.

## 2. EXPERIMENTAL METHOD

The data were obtained from a 100,000-picture exposure of the LRL 25-inch bubble chamber to a separated  $K^+$  beam at the Bevatron. The film was scanned twice for events with a vee or with more than two outgoing charged tracks. The topologies of interest here are vee plus one or two charged secondaries,

which are candidates for events of reaction (1), and three-prong events, which are candidates for the  $K^+ \rightarrow \pi^+ \pi^+ \pi^-$  decays used in the normalization. Initial measurements were made with the LRL Flying-Spot Digitizer, and remeasurements with Franckenstein measuring projectors. The measurements were passed through the programs SIOUX and ARROW. The  $K^+ d \rightarrow K^0 pp$  hypothesis is constrained even when one of the protons is too short to be visible. The cross sections were normalized to  $K^+ \rightarrow \pi^+ \pi^+ \pi^-$  decays, and corrections were made for  $K^0$  decay into neutral and long-lived decay modes,  $K^0$  decay outside the fiducial volume, and  $K^0$  decay too close to the production vertex. The scanning efficiency after two complete scans was better than 98%. About 4% of the events failed to pass any hypothesis after repeated measurement. This could usually be attributed to poor film quality or an obscured vertex. As scanning losses and measurement failures are small and appear to be independent of topology, no correction is necessary for them.

### 3. EXPERIMENTAL RESULTS

Cross sections for reaction (1) are given in table 1 and shown in fig. 1 together with results from other experiments at momenta below 3 GeV/c [4]. The cross section rises sharply from threshold to a value of about 7 mb at 600 MeV/c, remains roughly constant until about 900 MeV/c, and then falls smoothly, reaching 0.75 mb at 3 GeV/c. From 1.2 GeV/c up to the highest momentum reported, 12 GeV/c [5], the cross-section dependence on momentum is fit well by an expression of the form  $A p^{-n}$ , where  $A = 7.3 \pm 0.2$  mb and  $n = 2.10 \pm 0.05$ .

Values of the differential cross section for reaction (1) as a function of the momentum transfer from the incident  $K^+$  to the outgoing  $K^0$  are listed in table 1 and plotted in fig. 2. A substantial forward peak is present at

all momenta. The drop-off of  $d\sigma/dt$  at  $t = 0$  is at least in part due to the Pauli principle inhibition in the deuteron as discussed below.

#### 4. $K^+n$ ELASTIC CHARGE EXCHANGE

##### 4.1. General Considerations

It has been shown that, in the impulse and closure approximations, the  $K^+d$  charge exchange cross section  $(d\sigma/dt)_d$  [reaction (1)] is related to the neutron cross section  $(d\sigma/dt)_n$  [reaction (2)] by the formula [6]

$$\left(\frac{d\sigma}{dt}\right)_d = \left(\frac{d\sigma}{dt}\right)_n \left[ \frac{1 - H + (1 - \frac{H}{3})R}{1 + R} \right] \quad (3)$$

where  $R(t) = (d\sigma/dt)_n^{\text{spin flip}} / (d\sigma/dt)_n^{\text{nonspin flip}}$  and  $H(t)$  is a deuteron form factor. With the Hulthén wave function, the formula for  $H(t)$  is

$$H(t) = \frac{2\alpha\beta(\alpha + \beta)}{(\beta - \alpha)^2\sqrt{-t}} \left[ \tan^{-1} \frac{\sqrt{-t}}{2\alpha} + \tan^{-1} \frac{\sqrt{-t}}{2\beta} - 2 \tan^{-1} \frac{\sqrt{-t}}{\alpha + \beta} \right], \quad (4)$$

where the values  $\alpha = 45.6$  MeV and  $\beta = 7\alpha$  have been used. The function  $H(t)$  drops very rapidly from a value of unity at  $t = 0$ . Thus, over the whole angular range except very near the forward direction, formula (3) reduces very nearly to

$$\left(\frac{d\sigma}{dt}\right)_d = \left(\frac{d\sigma}{dt}\right)_n$$

Unfortunately near the forward direction, the deuteron correction is rather sensitive to the value of  $R$ ; consequently the very forward data give relatively little information about  $(d\sigma/dt)_n$ . The crosses in fig. 3 show the angular distributions obtained from  $(d\sigma/dt)_d$  by calculating the center-of-mass scattering angle between  $K^+$  and  $K^0$  in the system defined by the  $K^0$  and that proton which is faster in the laboratory. To obtain  $(d\sigma/dt)_n$  we have divided these data by the deuterium-correction factor on the right side of eq. (3) using three alternate assumptions,  $R = 0$ , 1, and  $\infty$ . Away from the forward direction, the three different corrected values

are nearly equal. However in the very forward direction ( $\cos \theta > 0.9$ ), they differ considerably, and we do not consider any conclusions reliable here.

We fit the corrected data for  $-1 \leq \cos \theta \leq 0.9$  to the series

$$\left(\frac{d\sigma}{d\Omega}\right)_n = \frac{\lambda^2}{4} \sum_{n=0}^{n_{\max}} A_n P_n(\cos \theta) \quad (5)$$

There is of course some arbitrariness as to the choice of  $n_{\max}$ , even within the rule that one should keep only as many orders as are necessary to give a reasonable fit. In figs. 3 and 4 the solid curves show fits, for the three values of  $R$ , corresponding to what we believe to be lower and upper limits for reasonable choices of  $n_{\max}$ . The 970, 1210 and 1365 MeV/c data give somewhat better fits with the high orders (fig. 4) whereas the 865 and 1585 MeV/c data are almost unaffected. Values of the Legendre coefficients and  $\chi^2$  for the fits corresponding to the middle curves ( $R = 1$ ) in figs. 3 and 4 are given in table 2 as sets A and B respectively and shown in fig. 5.\* Table 2 also shows the extrapolated forward differential cross sections and the corresponding optical values derived from the differences between  $K^+n$  and  $K^+p$  total cross sections. Although the experimental values of these forward cross sections are very sensitive to the value of  $n_{\max}$  and differ by large factors in the two sets of fits shown, they appear to be substantially greater than the optical values, indicating a largely real forward amplitude. The only momentum at which the lower-order fit (fig. 3) looks really poor is 1365 MeV/c. At this momentum the higher-order fit gives a rather different shape than for any of the other momenta, as well as a low forward cross section. We cannot tell whether this difference is due to a fluctuation or is a real effect;

---

\*The coefficients are sensitive to  $n_{\max}$  in spite of the orthogonality of Legendre polynomials because of the omission of the forward bin in the fit.



but, if real, it is probably well worth studying in more detail with large statistics. Other than reflecting the somewhat peculiar behavior at 1365 MeV/c, the Legendre coefficients exhibit as the main energy dependent feature a substantial rise in the coefficient  $A_1$ . In effect the principal change is an increasing peripheralism as the incident momentum increases.

#### 4.2. Regge Model

Fits to meson-nucleon charge exchange processes with Regge models have been presented in a number of papers [7, 8]. Generally such fits are expected to work only at high momenta (several GeV/c), but the presence at even low momenta of features characteristic of these high energy fits has suggested their extension to the low momentum region. In  $K^+n$  charge exchange these features include the peripheralism of the process, the reasonably smooth behavior as a function of momentum, and the reality of the forward amplitude.

Several years ago Rarita and Schwarzschild [8] attempted to include  $K^+n$  charge exchange at 2.3 GeV/c in an overall fit to meson-nucleon charge exchange and  $\eta$  production data. In addition to the usual  $\rho$  and  $A_2$  Regge trajectories, they introduced a  $\rho'$  term as an empirical method of parametrizing both the observed polarization in pion charge exchange and the rapid rise in the  $K^+$  charge exchange cross section as one goes to momenta below 3 GeV/c. Since the general qualitative features at 2.3 GeV/c do not change greatly as the momentum is decreased, it seems natural to attempt comparing the model with our low momentum data. Using the coefficients given by Rarita and Schwarzschild we obtain the dashed curves in fig. 2. With some modifications in the coefficients of the  $\rho'$  trajectory the solid curves of fig. 2 which give fairly good fits to the data are obtained.\* These modifications do not significantly affect fits to high energy K charge exchange data, other than slightly worsen the fit at 2.3 GeV/c.

\*In the notation of ref. 8, the following modifications have been made:  $D_{\rho}^0$  changed from 264 to 135 mb and  $D_{\rho}^1$ , changed from 2.95 to 2.30 (GeV/c)<sup>-2</sup>.

The agreement of the data with the Rarita-Schwarzschild model should not be interpreted as a real test of the model, but rather as an indication that the  $K^+n$  charge exchange angular distributions are fairly smooth functions of momentum down to rather low momenta.

#### 5. RESONANT $P_{1/2}$ INTERPRETATION

It has been suggested on the basis of total and inelastic cross-section data that there may be a very broad nearly elastic  $I = 0$  resonance near 1780 MeV [1]. The consequence of this idea would be the presence of a near-resonant elastic partial wave in the lower part of the momentum region that we are studying. The total cross-section measurements limit the size of the resonant cross section to  $4\pi\lambda^2$  and hence only the  $J = 1/2$  waves are possible candidates. Lower energy phase shift analyses indicate that the dominant  $I = 0$  partial wave is the  $P_{1/2}$ . The smallness of  $S_{1/2}$  relative to  $P_{1/2}$  tends to be confirmed by recent total cross-section measurements which indicate that the  $I = 0$  cross section falls to practically zero at zero momentum [3]. It thus appears that the  $P_{1/2}$  wave is the only real candidate for resonant behavior at low momentum.

We have attempted to fit our charge exchange data at 865 and 970 MeV/c, using the following additional inputs:

- (i) The  $I = 1$  phase shifts were taken as given in Hall et al. [9].
- (ii) The  $I = 0$  total cross sections of either  $20 \pm 1$  or  $23 \pm 1$  mb at 865 MeV/c and  $20.5 \pm 1$  or  $22.8 \pm 1$  <sub>mb</sub> at 970 MeV/c were taken to encompass the range of values obtained from the various experiments.

- (iii) The isospin-zero  $P_{1/2}$  phase shift is determined by the proposed resonance energy, 1780 MeV and width 560 MeV. The other phase shifts have been allowed to vary to obtain a best fit.

The results of this analysis are that no good fit can be obtained with our data and the inputs (i), (ii), (iii). The reason is fairly easy to see: a resonant  $P_{1/2}$  interfering with the dominant  $I = 1$ , negative  $S_{1/2}$  phase shift would lead to backward peaking in charge exchange, opposite to what is observed. This means that large amounts of other waves are needed to fix up this asymmetry. However, there is not much cross section room either in the  $I = 0$  total cross section or in the charge exchange cross section to add in these large contributions from other waves. Thus while it is true that the  $I = 0$  elastic process has a broad maximum at about 700 MeV/c, that maximum appears to contain significant contributions from a number of waves and is not caused by the  $P_{1/2}$  amplitude passing through  $90^\circ$ . It is possible however to obtain good fits with large  $P_{1/2}$  phase shifts, namely  $65^\circ$  and  $72^\circ$  at 865 and 970 MeV/c respectively instead of the values  $80^\circ$  and  $90^\circ$  expected for an elastic resonance of mass 1780 MeV and width 560 MeV. Examples of such fits are shown in table 3. In these fits, the reduction in  $P_{1/2}$  amplitude from that expected in the simple resonance interpretation provides enough room in the cross sections to accommodate D waves substantial enough to reverse the asymmetry and provide agreement with our experiment.

It is important to emphasize that we have not studied all possible phase shift solutions; and, indeed, that there are solutions with much smaller  $P_{1/2}$  phase shifts. Accurate polarization information is needed to distinguish the various solutions from each other, and such data are not presently available. Our only clear conclusion is that the  $P_{1/2}$  phase shift can be large, namely around  $65-72^\circ$  in the momentum range 800-1000 MeV/c, but it does not appear to follow the simple prescription of going through  $90^\circ$  in this momentum range. This does not rule out the existence of a  $P_{1/2}$  nearly elastic resonance below 1 GeV/c; it does however disagree with the simplest possible resonance interpre-

tation of the total cross-section data, namely a purely resonant elastic  $P_{1/2}$  partial wave.

We express our thanks to our scanning and measuring staff, to the operating staff of the Berkeley F.S.D. under Howard White, and to the crew of the 25-inch bubble chamber under Glenn Eckman.

#### REFERENCES

- [1] See, for example, G. Lynch, Hyperon Resonances - 70, edited by Earle Fowler (Moore Publishing Co., Durham, North Carolina, 1970), p. 9;  
R. L. Cool, ibid., p. 47;  
J. D. Dowell, ibid., p. 53;  
G. Goldhaber, ibid., p. 407.  
See also R. J. Abrams, R. L. Cool, G. Giacomelli, T. F. Kycia, K. K. Li and D. N. Michael, Phys. Letters 30B (1969) 564.
- [2] V. J. Stenger, W. E. Slater, D. H. Stork, H. K. Ticho, G. Goldhaber, and S. Goldhaber, Phys. Rev. 134 (1964) B1111;  
A. K. Ray, R. W. Burris, H. E. Fisk, R. W. Kraemer, D. G. Hill, and M. Sakitt, Phys. Rev. 183 (1969) 1183.
- [3] T. Bowen, P. K. Caldwell, F. N. Dikmen, E. W. Jenkins, R. M. Kalbach, D. V. Petersen, and A. E. Pifer, Phys. Rev. D2 (1970) 2599.
- [4] W. E. Slater, D. H. Stork, H. K. Ticho, W. Lee, W. Chinowsky, G. Goldhaber, S. Goldhaber, T. A. O'Halloran, Phys. Rev. Letters 7 (1961) 378;  
I. Butterworth, J. L. Brown, G. Goldhaber, S. Goldhaber, A. A. Hirata, J. A. Kadyk, B. M. Schwarzschild, and G. H. Trilling, Phys. Rev. Letters 15 (1965) 734, and unpublished data of the same authors;  
Y. Goldschmidt-Clermont, V. P. Henri, B. Jongejans, U. Kundt, F. Muller, R. L. Sekulin, M. Shafi, G. Wolf, J. M. Crispeels, J. Debaisieux, M. Delabaye,

- P. Dufour, F. Grard, J. Heughebaert, J. Naisse, G. Thill, R. Windmolders, K. Buchner, G. Dehm, G. Goebel, H. Hupe, T. Joldersma, I. S. Mittra, W. Wittek, *Physics Letters* 27B (1968) 602.
- [5] A. Firestone, G. Goldhaber, D. Lissauer, A. Hirata, and G. H. Trilling, *Phys. Rev. Letters* 25 (1970) 958.
- [6] B. M. Schwarzschild (Ph.D. thesis), Lawrence Radiation Laboratory Report UCRL-17572, June 1967 (unpublished).
- [7] B. J. Hartley, R. W. Moore and K. J. M. Moriarty, *Phys. Rev.* 187 (1969) 1921 and D1 (1970) 954.
- [8] W. Rarita and B. M. Schwarzschild, *Phys. Rev.* 162 (1967) 1378.
- [9] B. H. Hall, R. W. Bland, G. Goldhaber, and G. H. Trilling, Hyperon Resonances - 70, edited by E. C. Fowler (Moore Publishing Company, Durham, North Carolina, 1970), p. 435.

#### FIGURE CAPTIONS

- Fig. 1.  $\sigma(K^+d \rightarrow K^0pp)$  vs laboratory beam momentum. Data points below 865 MeV/c are from Slater et al. The data point at 2.3 GeV/c is from Butterworth et al. The data point at 3.0 GeV/c is from Goldschmidt-Clermont et al. [4].
- Fig. 2.  $d\sigma/dt$  vs  $-t$  for the five momenta of this experiment. The curves are the predictions of the Rarita-Schwarzschild model as discussed in the text.
- Fig. 3.  $(d\sigma/d\Omega)_d$  vs  $\cos \theta$  for the five momenta of this experiment. The curves are Legendre polynomial fits to  $(d\sigma/d\Omega)_n$  calculated from  $(d\sigma/d\Omega)_d$  using the correction factor of eq. (3) with  $R = 0, 1, \text{ and } \infty$ . The dots are  $(d\sigma/d\Omega)_n$  for  $R = 1$ . The fits at 865, 970, and 1210 MeV/c are to second order, at 1365 and 1585 to third order. The forwardmost bin was omitted in these fits.
- Fig. 4. Same as fig. 3 but the fits are to higher order; to fourth order at 865, 970, and 1210 MeV/c; to fifth order at 1365 and 1585 MeV/c.
- Fig. 5. The expansion coefficients for the fits in figs. 3 and 4. The open circles correspond to Set A in table 2 and fig. 3; the closed circles correspond to Set B in table 2 and fig. 4.

Table 1. Differential cross sections for  $K^+d \rightarrow K^0p(p)$ ;  $t$  is the square of the momentum transfer from the incident  $K^+$  to the outgoing  $K^0$ .

-t interval (GeV/c) <sup>2</sup>		Cross sections				
From	To	$P_K = 865 \text{ MeV/c}$	970	1210	1365	1585
All		$\sigma = 6.72 \pm 0.40 \text{ mb}$	$6.26 \pm 0.29$	$4.99 \pm 0.24$	$3.69 \pm 0.29$	$2.65 \pm 0.22$
0.00	0.05	$4.6 \pm 1.1$	$4.3 \pm 0.8$	$2.7 \pm 0.6$	$3.1 \pm 0.6$	$1.9 \pm 0.4$
0.05	0.10	$9.3 \pm 1.6$	$6.2 \pm 0.9$	$5.7 \pm 0.9$		
0.10	0.15	$11.5 \pm 1.7$	$7.8 \pm 1.0$	$6.7 \pm 1.0$	$3.8 \pm 0.7$	$3.1 \pm 0.6$
0.15	0.20	$10.6 \pm 1.7$	$10.3 \pm 1.2$	$6.5 \pm 0.9$		
0.20	0.25	$9.3 \pm 1.5$	$10.4 \pm 1.2$	$6.0 \pm 0.9$	$4.5 \pm 0.8$	$3.4 \pm 0.6$
0.25	0.30	$9.4 \pm 1.6$	$9.2 \pm 1.1$	$5.5 \pm 0.8$		
0.30	0.35	$11.8 \pm 1.8$	$7.6 \pm 1.0$	$6.3 \pm 0.9$	$4.0 \pm 0.7$	$4.0 \pm 0.7$
0.35	0.40	$8.6 \pm 1.5$	$6.6 \pm 0.9$	$6.1 \pm 0.9$		
0.40	0.45	$8.0 \pm 1.4$	$6.6 \pm 0.9$	$5.2 \pm 0.8$	$3.9 \pm 0.7$	$1.4 \pm 0.4$
0.45	0.50	$8.1 \pm 1.4$	$6.3 \pm 0.9$	$3.6 \pm 0.7$		
0.50	0.55	$8.7 \pm 1.5$	$5.3 \pm 0.8$	$5.0 \pm 0.8$	$2.9 \pm 0.6$	$1.3 \pm 0.4$
0.55	0.60	$6.1 \pm 1.2$	$5.6 \pm 0.9$	$4.6 \pm 0.8$		
0.60	0.65	$4.6 \pm 1.1$	$5.2 \pm 0.8$	$2.8 \pm 0.6$	$1.8 \pm 0.5$	$1.6 \pm 0.4$
0.65	0.70	$6.1 \pm 1.2$	$4.5 \pm 0.8$	$3.6 \pm 0.7$		
0.70	0.75	$6.4 \pm 1.3$	$4.4 \pm 0.8$	$3.2 \pm 0.6$	$2.0 \pm 0.5$	$1.1 \pm 0.4$
0.75	0.80	$3.5 \pm 0.9$	$5.1 \pm 0.8$	$3.1 \pm 0.6$		
0.80	0.85	$3.2 \pm 0.9$	$4.4 \pm 0.8$	$2.7 \pm 0.6$	$1.4 \pm 0.4$	$1.3 \pm 0.4$
0.85	0.90	$1.8 \pm 0.7$	$4.5 \pm 0.8$	$2.3 \pm 0.5$		
0.90	0.95	$1.3 \pm 0.6$	$2.8 \pm 0.6$	$2.6 \pm 0.6$	$1.2 \pm 0.4$	$0.65 \pm 0.27$
0.95	1.00	$1.2 \pm 0.6$	$3.0 \pm 0.6$	$2.4 \pm 0.5$		
1.00	1.05	$0.12 \pm 0.09$	$2.0 \pm 0.5$	$1.9 \pm 0.5$	$1.4 \pm 0.4$	$0.92 \pm 0.31$
1.05	1.10		$1.0 \pm 0.4$	$1.2 \pm 0.4$		
1.10	1.15		$0.64 \pm 0.29$	$1.3 \pm 0.4$	$1.8 \pm 0.5$	$0.92 \pm 0.31$
1.15	1.20		$0.51 \pm 0.25$	$1.6 \pm 0.4$		
1.20	1.25		$0.25 \pm 0.18$	$1.1 \pm 0.4$	$1.8 \pm 0.5$	$0.62 \pm 0.25$
1.25	1.30	$0.39 \pm 0.22$	$1.3 \pm 0.4$			
1.30	1.35	$0.14 \pm 0.10$	$1.2 \pm 0.4$	$1.2 \pm 0.4$	$0.83 \pm 0.23$	$0.73 \pm 0.28$
1.35	1.40		$0.95 \pm 0.34$	$0.95 \pm 0.34$		
1.40	1.50		$0.49 \pm 0.17$	$0.49 \pm 0.17$	$0.64 \pm 0.20$	$0.41 \pm 0.15$
1.50	1.60	$0.30 \pm 0.14$	$0.30 \pm 0.14$			
1.60	1.70	$0.05 \pm 0.02$	$0.05 \pm 0.02$	$0.05 \pm 0.02$	$0.08 \pm 0.04$	$0.37 \pm 0.14$
1.70	1.80					
1.80	1.90					
1.90	2.00					
2.00	2.10					
2.10	2.20	$0.05 \pm 0.02$	$0.05 \pm 0.02$	$0.05 \pm 0.02$	$0.08 \pm 0.04$	$0.35 \pm 0.13$
2.20	2.30					
2.30	2.90					

Table 2. Coefficients  $A_n$  from the least squares fit of the differential cross sections to the series  $(d\sigma/d\Omega)_n = (d\sigma/d\Omega)_d / (1-2/3H) = \frac{\lambda^2}{4} \sum_{n=0}^{n_{\max}} A_n P_n(\cos \theta)$ .

The forwardmost bin ( $0.9 < \cos \theta \leq 1.0$ ) has not been included in the fit.

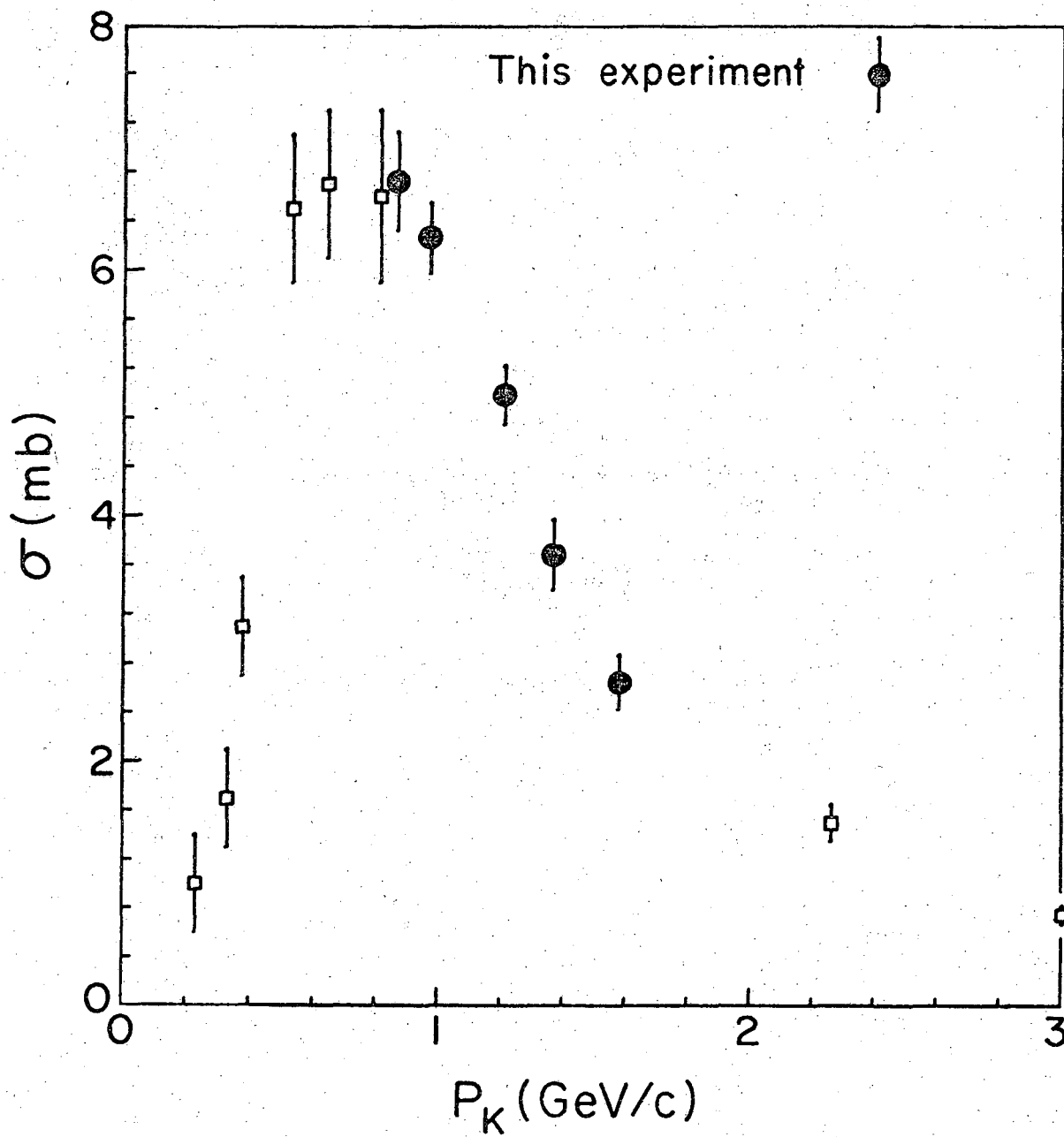
Beam momentum (MeV/c)	$n_{\max}$	$\chi^2$	Expected $\chi^2$	Probability (%)	$A_0$	$A_1$	$A_2$	$A_3$	$A_4$	$A_5$	$(d\sigma/d\Omega)_{\theta=0}$ (mb/sr)	$(d\sigma/d\Omega)_{\text{optical}}$ (mb/sr)
865	2	16.8	16	39.9	1.27±0.06	0.57±0.11	-0.18±0.13				0.74±0.10	0.02±0.02
970	2	31.4	16	1.2	1.39±0.05	0.70±0.09	0.12±0.11				0.83±0.07	0.02±0.02
Set A 1210	2	9.5	16	89.1	1.58±0.06	1.43±0.12	0.31±0.12				0.90±0.07	0.03±0.02
1365	3	13.6	13	40.5	1.41±0.09	1.48±0.18	0.88±0.23	0.77±0.22			1.04±0.13	0.01±0.02
1585	3	8.9	15	88.3	1.20±0.08	1.60±0.18	1.00±0.22	0.40±0.20			0.78±0.11	0.01±0.02
-----												
865	4	16.0	14	31.2	1.28±0.06	0.56±0.13	-0.15±0.17	0.04±0.21	-0.11±0.21		0.72±0.27	0.02±0.02
970	4	22.2	14	7.4	1.35±0.05	0.57±0.10	-0.12±0.14	-0.38±0.17	-0.49±0.17		0.35±0.18	0.02±0.02
Set B 1210	4	6.3	14	95.9	1.55±0.07	1.35±0.14	0.19±0.19	-0.22±0.22	-0.33±0.19		0.68±0.18	0.03±0.02
1365	5	6.1	11	86.7	1.29±0.10	1.07±0.24	0.18±0.35	-0.20±0.41	-1.13±0.41	-0.60±0.32	0.14±0.36	0.01±0.02
1585	5	8.7	13	79.2	1.19±0.10	1.56±0.24	0.93±0.34	0.32±0.39	-0.10±0.38	-0.12±0.30	0.71±0.29	0.01±0.02

Table 3.  $K^+N$   $I = 0$  phase shifts ( $\delta$ ), inelasticity coefficients ( $\eta$ ), and partial cross sections for the momenta 865 and 970 MeV/c. Set of solutions corresponding to large  $P_{1/2}$  waves. For the  $I = 1$  phase shifts we used the set reported at the Duke Conference by Hall et al. <sup>9</sup>

	Wave	$\delta$ (deg)	$\eta^a$	$\sigma^0$ el (mb)	$\sigma^0$ inel (mb)
865 MeV/c	$S_{1/2}$	$-12.7 \pm 5.9$	0.980	1.06	0.22
	$P_{1/2}$	$65.2 \pm 2.5$	0.984	18.03	0.17
	$P_{3/2}$	$5.3 \pm 3.6$	0.992	0.37	0.17
	$D_{3/2}$	$9.4 \pm 2.2$	0.989	1.17	0.24
	$D_{5/2}$	$-7.1 \pm 3.4$	0.994	<u>1.02</u>	<u>0.20</u>
				Totals	21.65
$\sigma^0_{\text{total}}$ from fit		= 22.7 mb	$\chi^2 = 25.4$ for 18 DOF		
970 MeV/c	$S_{1/2}$	$-6.6 \pm 3.9$	0.944	0.25	0.51
	$P_{1/2}$	$72.2 \pm 5.0$	0.926	15.73	0.67
	$P_{3/2}$	$10.1 \pm 4.4$	0.969	1.12	0.57
	$D_{3/2}$	$13.8 \pm 3.3$	0.981	2.09	0.35
	$D_{5/2}$	$-10.7 \pm 2.9$	0.987	<u>1.92</u>	<u>0.35</u>
				Totals	21.11
$\sigma^0_{\text{total}}$ from fit		= 23.5 mb	$\chi^2 = 26.2$ for 18 DOF		

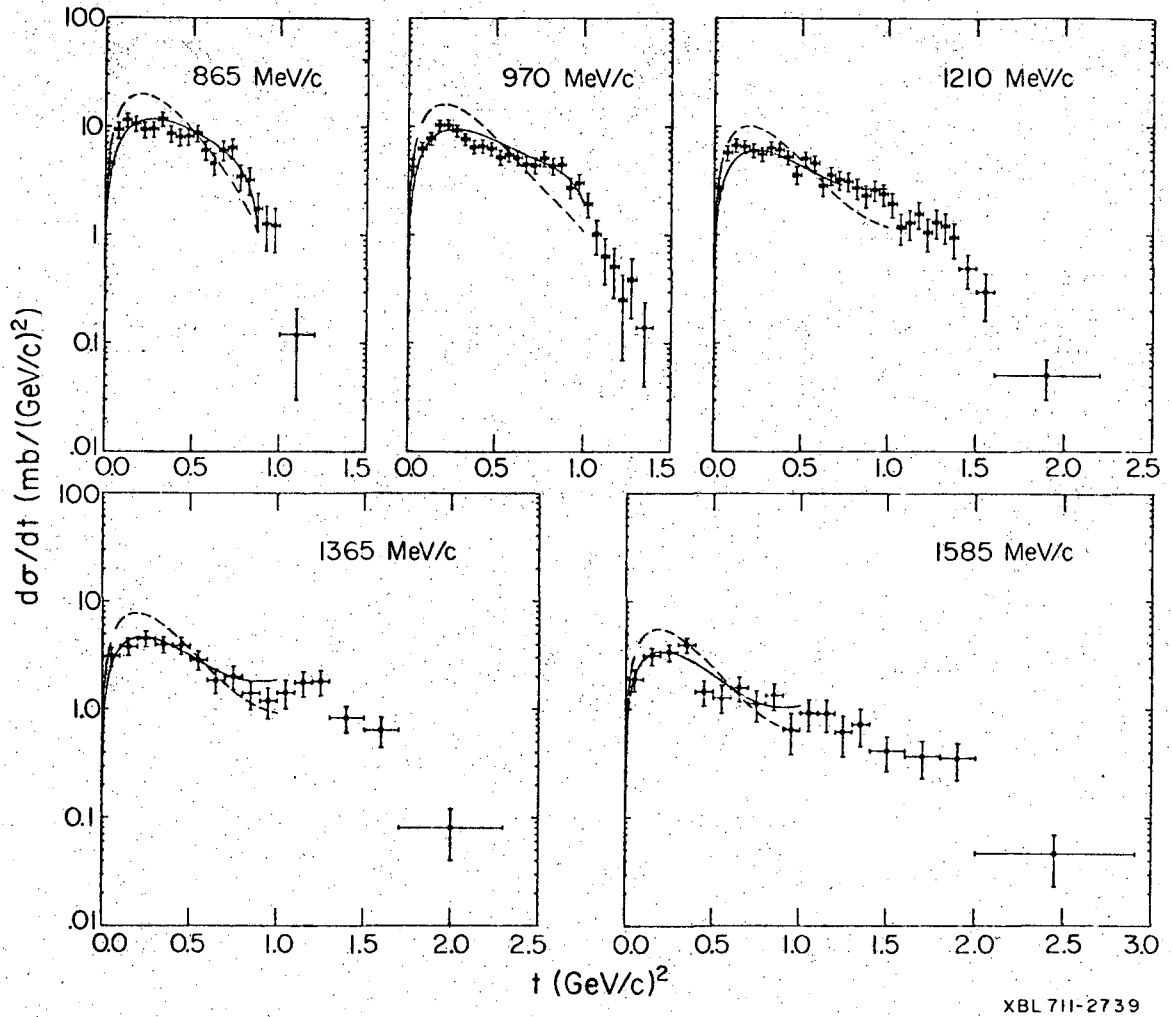
a) The quantities  $\eta$  were chosen in similar ratios as obtained for the corresponding  $I = 1$  solutions. The fitting program was allowed to vary them within limits with the constraint that  $\sum_j \sigma^0_{\text{inel}}(j) = \sigma^0_{\text{inel}} \text{ expt.}$





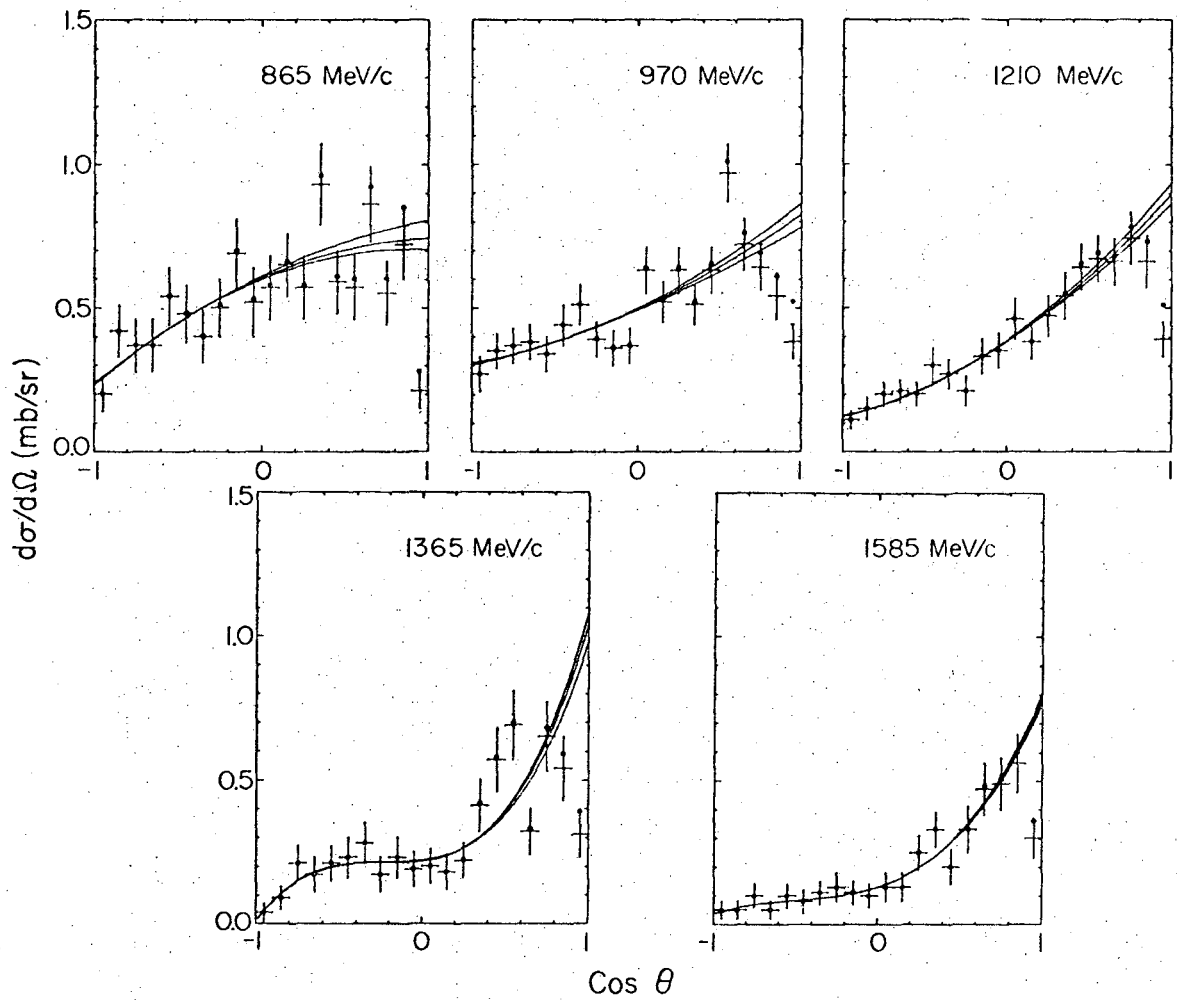
XBL711-2741

Fig. 1



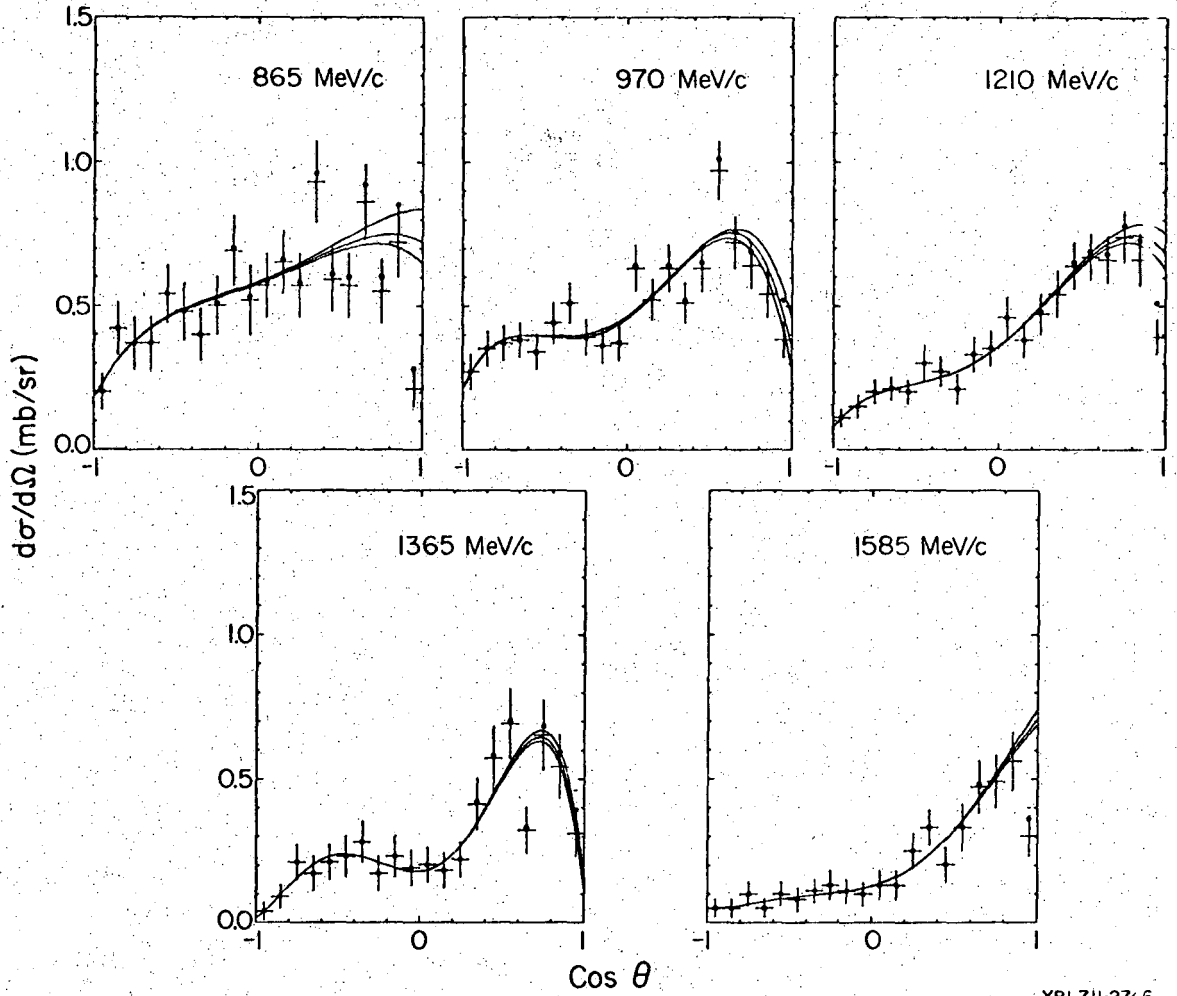
XBL 711-2739

Fig. 2



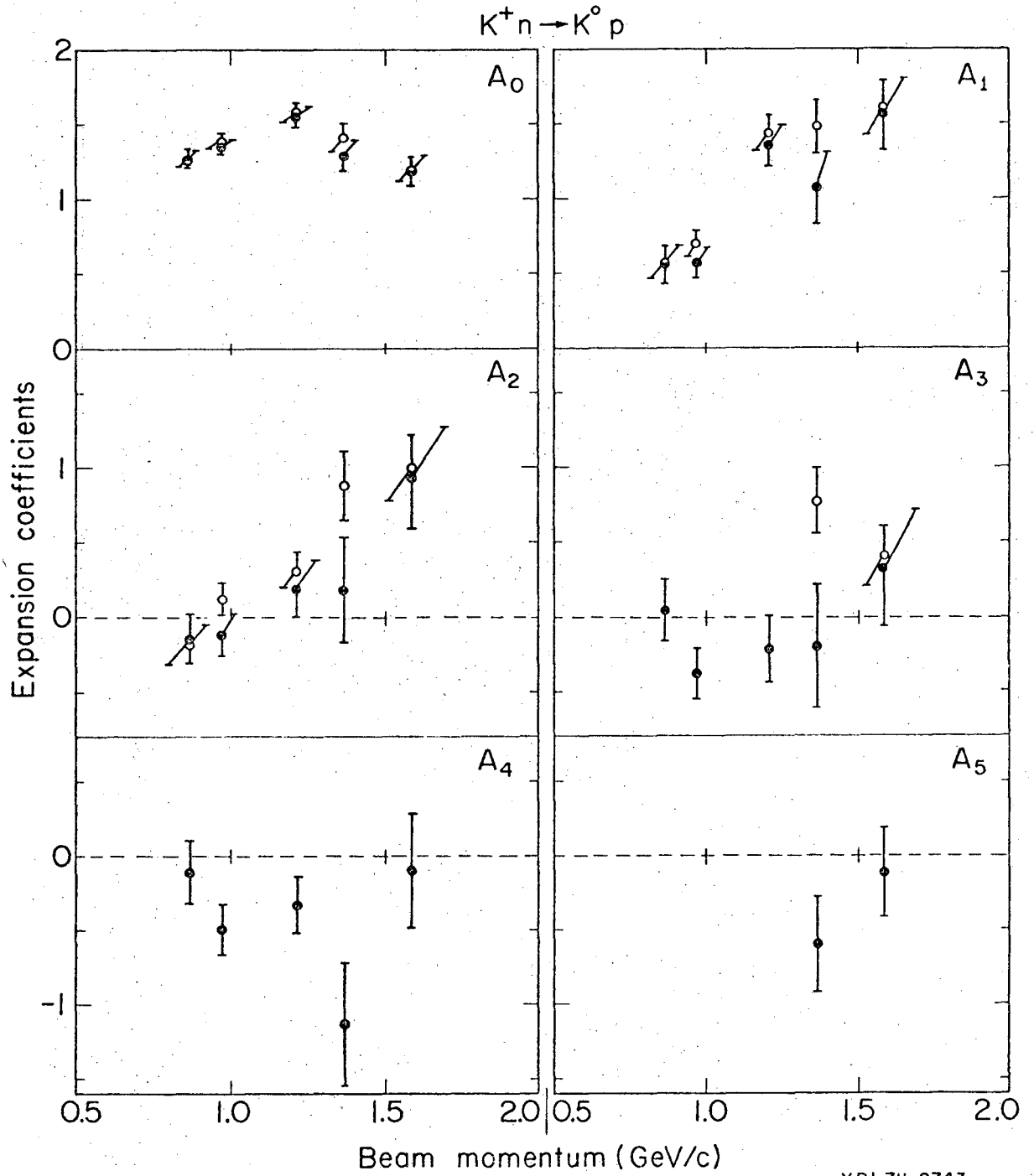
XBL 711-2740

Fig. 3



XBL711-27-6

Fig. 4



XBL7II-2743

Fig. 5

LEGAL NOTICE

*This report was prepared as an account of work sponsored by the United States Government. Neither the United States nor the United States Atomic Energy Commission, nor any of their employees, nor any of their contractors, subcontractors, or their employees, makes any warranty, express or implied, or assumes any legal liability or responsibility for the accuracy, completeness or usefulness of any information, apparatus, product or process disclosed, or represents that its use would not infringe privately owned rights.*

TECHNICAL INFORMATION DIVISION  
LAWRENCE RADIATION LABORATORY  
UNIVERSITY OF CALIFORNIA  
BERKELEY, CALIFORNIA 94720